JOURNAL OF COMPUTATIONAL PHYSICS 10, 1–21 (1972)

Numerical Solution of Quasi-Conservative Hyperbolic Systems—The Cylindrical Shock Problem*

S. ABARBANEL AND M. GOLDBERG

Department of Mathematical Sciences, Tel-Aviv University, Tel-Aviv, Israel

Received January 27, 1971

In this paper we consider the numerical solution of hyperbolic systems of partial differential equations which are in quasi-conservation form. A basic Lax–Wendroff-like scheme is developed. In order to treat problems with discontinuous solutions an iterative procedure is proposed. The stability and convergence of the various schemes are investigated. It is shown that it is possible to have time steps considerably larger than those allowed according to the CFL (Courant–Friedricks–Levy) criterion.

The method is then applied to the case of converging–diverging cylindrical shock waves. Detailed behavior near the axis at the time of shock coalescence is obtained, as well as the general flow field at various times. The results are compared with Payne [4] and the differences are pointed out.

The computations reported herein were carried out on the CDC-3400 computer at the Tel-Aviv University computation center.

1. INTRODUCTION

In general the hydrodynamic-time-dependent inviscid, compressible flow equations can be written as a hyperbolic system of partial differential equations cast in conservation form [1]. That this is so for general curvilinear coordinates has been shown by Anderson *et al.* [2]. There are, however, cases of physical interest which cannot be put into conservation form. For example the nonlinear shallow fluid flow problem [3][1], and in general problems of cylindrical or spherical symmetry. A particular case is that of the problem of converging shock waves. This problem was treated by Payne [4] and serves as a good test case for the methods developed herein.

* This Research has been sponsored in part by the Air Force Office of Scientific Research (NAM) through the European Office of Aerospace Research, AFSC, United States Air Force, under contract F61052-69-C-0041.

[1] In the paper by Houghton and Kasahara a particular problem is formulated and analyzed. In the present work we begin by formulating and analyzing the general case and then apply the results to a specific physical case.

We are interested then in the numerical integration of hyperbolic systems of the form

$$W_t + [F(W)]_x = \psi(x; W) \tag{1.1}$$

where the independent variables are x and t; W is a vector of k components $(W_1, ..., W_k)$ which are unknown scalar functions of x and t. $F = F(W) \equiv F(W_1, ..., W_k)$ and $\psi = \psi(W; x) \equiv \psi(W_1, ..., W_k; x)$ are also k dimensional vectors. We say that Eq. (1.1) is in a "quasi-conservation" form, because the R.H.S. does not contain any derivatives. If ψ did depend explicitly on t we could with very little difficulty extend the results to be given in this work.

2. Difference Methods for Quasi-Conservative Hyperbolic Systems

2a. *The Basic Difference Scheme*

Consider the quasilinear inhomogeneous hyperbolic system of k partial differential equations given in the form

$$\frac{\partial W}{\partial t} + A \frac{\partial W}{\partial x} = \psi(W; x), \tag{2.1}$$

where A is a $k \times k$ matrix whose components are functions of $(W_1, ..., W_k)$. A is the Jacobian of $F(W)$ in (1.1) with respect to the vector W, i.e., $A_{ij} = \partial F_i / \partial W_j$. The hyperbolicity of the system is assured by requiring the eigenvalues of A to be real. We are interested in obtaining a solution valid in the region

$$\mathscr{D} = \{0 \leqslant x \leqslant X, 0 \leqslant t \leqslant T\},$$

with appropriate initial and boundary conditions assuming, of course, that the problem is well posed.

The difference scheme which approximates (2.1) is developed in the manner of Lax and Wendroff [1], i.e., it is based upon a Taylor series of W in time. Assuming W to possess derivatives to third order in $\mathscr{D}$ we have

$$W(x, t + \Delta t) = W(x, t) + \Delta t \cdot W_t + \frac{(\Delta t)^2}{2!} \cdot W_{tt} + O[(\Delta t)^3]. \tag{2.2}$$

The time derivatives may be represented as space derivatives by using (1.1) and (2.1). With simple manipulations, Eq. (2.2) becomes

$$W(x, t + \Delta t) = W(x, t) - (\Delta t) \cdot F_x + \frac{(\Delta t)^2}{2} (AF_x)_x + \Delta t \left\{ \psi + \frac{\Delta t}{2} [\psi_t - (A\psi)_x] \right\} + O[(\Delta t)^3] \tag{2.3}$$

We see that when $\psi \equiv 0$ we get back the Lax–Wendroff scheme for the strictly conservation-form case. For the difference equation corresponding to (2.3) we take

$$W_j^{n+1} = W_j^n + QW_j^n + (\Delta t)\,\tilde{Q}W_j^n, \tag{2.4}$$

where

$$W_j^n \equiv W(j\,\Delta x, n\,\Delta t) = W(x_j, t_n), \tag{2.5}$$

$$QW_j^n = -\frac{\lambda}{2}[F_{j+1}^n - F_{j-1}^n] + \frac{\lambda^2}{2}[A_{j+1/2}^n(F_{j+1}^n - F_j^n) - A_{j-1/2}^n(F_j^n - F_{j-1}^n)], \tag{2.6}$$

$$\tilde{Q}W_j^n = \psi_j^n + \left(\frac{\Delta t}{2}\right)(\psi_t)_j^n - \frac{\lambda}{4}[(A\psi)_{j+1}^n - (A\psi)_{j-1}^n], \tag{2.7}$$

with

$$\lambda = \frac{\Delta t}{\Delta x}; \qquad [f(W)]_j^n = f_j^n,$$

and where the m-th component of ψ_t is easily found to be

$$[(\psi_m)_t]_j^n = \sum_{l=1}^{k}\left(\frac{\partial \psi_m}{\partial W_l}\right)_j^n \left\{-\frac{1}{2\Delta x}[(F_l)_{j+1}^n - (F_l)_{j-1}^n] + (\psi_l)_j^n\right\}. \tag{2.8}$$

Note that to second order accuracy,

$$A_{j\pm 1/2}^n \equiv A(W_{j\pm 1/2}^n) = A[\tfrac{1}{2}(W_{j\pm 1}^n + W_j^n)]. \tag{2.9}$$

Since (2.6) is the Lax–Wendroff difference operator, accurate to second order, and since (2.7) is built up of centered differences only, it follows that our difference scheme (2.4) is of second order accuracy.

As usual, the stability of the difference scheme can be investigated only in the linear sense. To do this we assume that A and ψ are locally constant and under these circumstances we may rewrite (2.4) as follows:

$$W_j^{n+1} = SW_j^n + \Delta t\psi, \tag{2.10}$$

where S is the linear Lax–Wendroff operator, given by

$$SW_j^n = W_j^n - \frac{\lambda A}{2}(W_{j+1}^n - W_{j-1}^n) + \frac{\lambda^2 A^2}{2}(W_{j+1}^n - 2W_j^n + W_{j-1}^n). \tag{2.11}$$

Note that (2.10) has the form of an affine transformation. Its stability can be proven in a manner very similar to that by which Kreiss [6] and Strang [7] prove the stability of a scheme similar to (2.10) but with $\Delta t\psi$ replaced by $\Delta t H(W_j^n)$ with

H being a bounded linear operator. The proof in the present case is straightfoward and is omitted here.

To summarize, the linear stability of (2.4) is assured by meeting the CFL criterion (which is satisfied by the Lax–Wendroff scheme)

$$\frac{\Delta t}{\Delta x} \leqslant \frac{1}{\rho(A)}, \tag{2.12}$$

where $\rho(A)$ is the spectral radius of A. The convergence of the difference scheme can be easily demonstrated by using the methods delineated by Richtmyer and Morton [8].

2b. *Iterative Difference Schemes*

A difference scheme such as (2.4), or others which are in use, are quite satisfactory from the numerical point of view when one deals with problems possessing smooth solutions. When, however, the solution contains discontinuities the numerical procedure yields oscillations which can be quite strong in the neighborhood of a discontinuity such as that representing a shock wave. These post-shock oscillations may in time distort the true solution. There are several methods to overcome this phenomenon. Most of them consist of adding certain terms (often called artificial viscosity [1, 8]) to the basic scheme. These terms often reduce the amplitude and duration of the nonlinear instabilities which we called post-shock oscillations. A different approach was taken by Abarbanel and Zwas [5] and yielded, in the case of slab symmetry, smooth monotonic shock profiles for a large range of the controlling physical parameters. It will be shown later that a modification of this iterative scheme will yield good results also in the present quasi-conservation case.

To delineate the method we start by considering the following general explicit difference scheme:

$$W_j^{n+1} = (I + C)\, W_j^n = W_j^n + CW_j^n, \tag{2.13}$$

where C is any difference operator accurate at least to order two. For example in in our case of (2.4) $C = Q + \Delta t\tilde{Q}$. Next examine the following explicit–implicit difference equation

$$\begin{aligned} W_j^{n+1} &= W_j^n + (1 - \theta)\, CW_j^n + \theta CW_j^{n+1} \\ &= W_j^n + CW_j^n + \theta[CW_j^{n+1} - CW_j^n], \end{aligned} \tag{2.14}$$

where θ is a real number. When $\theta = 0$ we get back the basic difference Eq. (2.13). Based on (2.14) we introduce the notion of an iterative scheme in which the results

of $(s-1)$ iterations are designated by $W^{n,s}$. The iterated vector W satisfies the following recursion relation

$$\begin{aligned} W^{n+1,s+1} &= W_j^n + [(1-\theta)\, CW_j^n + \theta CW_j^{n+1,s}] \\ &= W_j^n + CW_j^n + \theta[CW_j^{n+1,s} - CW_j^n] \end{aligned} \tag{2.15}$$

where $s = 0, 1, \ldots, l-1$ and

$$W_j^{n+1,0} \equiv W_j^n. \tag{2.16}$$

Notice that when $l = 1$ or $s = 0$ (i.e., no iteration) the result reverts back to the basic scheme (2.13). It should be remarked here that (2.15) differs somewhat from the scheme proposed in Ref. [5]. There the corresponding equation reads as follows:

$$W^{n+1,s+1} = W_j^n + C[(1-\theta)\, W_j^n + \theta W_j^{n+1,s}]. \tag{2.17}$$

When C is a linear difference operator, (2.15) and (2.17) are identical. In general, however, they are not. We shall in what follows refer to (2.15) and (2.17), respectively, as the "external" and "internal" iterative schemes. The names allude to positioning of θ with respect to the operator C. With regard to the stability and convergence analyses of the iterative method it does not matter whether we use the "external" or "internal" scheme. This is so because in order to carry out the analyses, we have to assume local constancy of the operator C. In our specific case $C = Q + \Delta t\tilde{Q}$. But under the assumptions of local constancy

$$CW_j^n = (S - I)\, W_j^n + \Delta t\psi$$

(see Eqs. (2.4) and (2.10)). While the operator C under these restrictions is not a linear operation (but an affine one) it can be shown that it still satisfies the relation

$$C[(1-\theta)\, W_j^n + \theta W_j^{n+1,s}] = (1-\theta)\, CW_j^n + \theta CW_j^{n+1,s}. \tag{2.18}$$

Specifically we consider the linear stability of the scheme

$$W_j^{n+1} = W_j^n + \tilde{S}W_j^n + \Delta t\psi, \tag{2.19}$$

where the linear operator $\tilde{S} = S - I$ with S given by (2.11) and ψ is assumed a constant vector. It follows from (2.15) (or (2.17)) that the iterative procedure here takes the form

$$W_j^{n+1,s+1} = W_j^n + \tilde{S}[\theta W_j^{n+1,s} + (1-\theta)\, W_j^n] + \Delta t\psi. \tag{2.20}$$

If we designate the final result after performing l iterations by $w_j^{n+1,l} \equiv w_j^{n+1}$, and use an analysis very similar to that of Ref. [5], then our scheme becomes

$$w_j^{n+1} \equiv w_j^{n+1,l} = \left[1 + (1 + \mu) \sum_{r=1}^{l} \Omega^r\right] w_j{}^n + \Delta t \psi \tag{2.21}$$

where the linear operator Ω is defined by

$$\Omega f_j{}^n = -\frac{\lambda\theta\Omega}{2}(f_{j+1}^n - f_{j-1}^n) + \frac{\lambda^2 A^2\theta^2}{2}(f_{j+1}^n - 2f_j{}^n + f_{j-1}^n) \tag{2.22}$$

and f is a vector function of the correct dimension. The linear stability of (2.21) is assured with the stability of the operator $1 + (1 + \mu)\sum_{r=1}^{l} \Omega^r$. The corresponding amplification matrix is given by (see Ref. [5])

$$G = G(\Delta t, \omega) = 1 + (1 + \mu) \sum_{r=1}^{l} (D + iB)^r, \tag{2.23}$$

where the matrices D and B are

$$D = -2\lambda^2\theta A^2 \sin^2 \phi,$$
$$B = -\lambda\theta A \sin 2\phi,$$

with $\phi = \omega\Delta x/2$; ω being the wave number.

By the spectral mapping theorem the eigenvalues of G are given by

$$\begin{aligned} g &= 1 + (1 + \mu) \sum_{r=1}^{l} (d + ib)^r \\ &= -\mu + (1 + \mu) \sum_{r=0}^{l} (d + ib)^r \\ &= -\mu + (1 + \mu)[1 - (d + ib)^{l+1}]/[1 - (d + ib)], \end{aligned} \tag{2.24}$$

where, from the definitions of D and B,

$$\begin{aligned} d &= -2\lambda^2\theta a^2 \sin^2 \phi, \\ b &= -\lambda\theta a \sin 2\phi, \end{aligned} \tag{2.25}$$

and a is the corresponding eigenvalue of A. The condition $|g| \leqslant 1$ cannot be solved analytically except for special values of ϕ and μ. These special cases served as a check on the numerical solution of | R.H.S. of (2.24)| $\leqslant 1$. The results may be summarized as follows:

(1) $\theta < 0 (\mu < 0)$. The scheme (2.21), is unconditionally unstable.

(2) $\theta = 0$; $\theta > 1 (\mu < 0)$; $\frac{1}{2} \leqslant \theta \leqslant 1 (\theta \leqslant \mu \leqslant 1)$. In all of these cases the stability conditions are bounded by the CFL one. In fact a stability condition as good as CFL (i.e., $\lambda \leqslant 1/\rho(A)$) is achieved only for $\theta = 1/2$, and $\theta = 0$. (In the latter case, scheme (2.21) reverts back to the Lax–Wendroff operator).

(3) $0 < \theta \leqslant \frac{1}{2} (\mu > 1)$. In this range it is quite complicated to draw conclusions from the numerical solution of (2.24); however, one also gets the most advantageous results in this range. First recall that as $\theta = 1/2$ or $\theta \to 0$ we return to the CFL case. Again we distinguish between two cases:

(i) When l is even there exists $0 < \theta_0(l) < \frac{1}{2}$ such that in the interval $[\theta_0(l) \leqslant \theta \leqslant 1/2]$ the stability criterion is

$$\lambda = (\Delta t/\Delta x) \leqslant 1/(\rho(A)\sqrt{2\theta}). \tag{2.26}$$

As $l \to \infty$, $\theta_0(l) \to \frac{1}{2}$ so that the interval contracts monotonically with l. In the remaining interval $(0 < \theta < \theta_0(l))$ the stability criterion is more restricted and is given by

$$\begin{aligned} &\lambda = (\Delta t/\Delta x) \leqslant [z(\theta, l)/\rho(A)], \\ &1 \leqslant z(\theta, l) \leqslant 1/\sqrt{2\theta_0}\,. \end{aligned} \tag{2.27}$$

(ii) When l is odd, we have

$$\lambda = (\Delta t/\Delta x) \leqslant [\tilde{z}(\theta, l)/\rho(A)], \tag{2.28}$$

with

$$1 \leqslant \tilde{z}(\theta, l) \leqslant 1/\sqrt{2\theta}.$$

The significance of case (3i) can be seen from the fact that if $l = 2$, then $0.165 < \theta_0 < 0.175$; if $l = 4$, $0.2 < \theta_0 < 0.3$, etc. Thus if we take $l = 2$ and choose $\theta = 0.2$ the stability condition becomes

$$\lambda = (\Delta t/\Delta x) \leqslant [1/\rho(A)\sqrt{0.4}] \approx [1.58/\rho(A)]. \tag{2.29}$$

Thus we are allowed to use time steps which are about 60% larger than those allowed by the CFL condition. It should be emphasized that these theoretical results were applied successfully to actual hydrodynamical problems.

In any case it is clear that for $0 < \theta < 1/2$ and for any l one can exceed the CFL or other condition suitable for the other ranges of θ. The explanation for these seemingly paradoxical results (i.e., improvement upon CFL) lies in the fact that the iterations cause the scheme to be anchored not only on $j + 1, j$ and $j - 1$ but on $j + l, j + l - 1, \ldots, j, \ldots, j - l + 1, j - l$. In other words, the numerical domain of influence has been increased.

The iterations converge in the limit $l \to \infty$ to the implicit scheme, i.e.,

$$W_j^{n+1} = W_j^n + (1 - \theta)\, CW_j^n + \theta CW_j^{n+1}. \tag{2.30}$$

The proof, done for the case with locally constant operator, is almost the same as that given in Ref. [5]. The important result is that in the range $0 < \theta < 1$ the stability criterion is more severe. Thus stability of the scheme assures convergence.

3. Applications to Cylindrical Shock Waves

3.a *The Hydrodynamic Equations*

We are considering a compressible, inviscid, non-heat-conducting polytropic fluid. If we assume either slab, cylindrical or spherical symmetry of the flow the equations of motion take the following form [8]:

$$W_t + [F(W)]_r = \psi(W, r) \tag{3.1}$$

with

$$W = \begin{pmatrix} R \\ M \\ E \end{pmatrix}; \qquad F = \begin{pmatrix} M \\ (\gamma - 1)\, E + \dfrac{3 - \gamma}{2}\left(\dfrac{M^2}{R}\right) \\ \dfrac{M}{R}\left[\gamma E - (\gamma - 1)\,\dfrac{M^2}{2R}\right] \end{pmatrix},$$

$$\psi = \frac{(\gamma - 1)(\alpha - 1)}{r}\begin{pmatrix} 0 \\ E - \dfrac{M^2}{2R} \\ 0 \end{pmatrix} = (\gamma - 1)\, r^{\alpha - 2}\begin{pmatrix} 0 \\ p \\ 0 \end{pmatrix}, \tag{3.2}$$

and

$$R = r^{\alpha-1}\rho; \qquad M = r^{\alpha-1}\rho u \equiv r^{\alpha-1}m; \qquad E = r^{\alpha-1}\rho\left(\epsilon + \frac{u^2}{2}\right) \equiv r^{\alpha-1}e, \tag{3.3}$$

where ρ, u, ϵ, p, t and r are, respectively, the fluid density, particle velocity, internal energy per unit mass, pressure, time and the space coordinate of symmetry. Thus when $\alpha = 1$ we have slab symmetry and $r = x$. When $\alpha = 2, 3$ we have, respectively, cylindrical or spherical symmetry and r is the radius. In (3.2) and (3.3) we used the polytropic equation of state $p = (\gamma - 1)\,\rho\epsilon$ in the form

$$p = \frac{\gamma - 1}{r^{\alpha-1}}\left(E - \frac{M^2}{2R}\right) = (\gamma - 1)\left(e - \frac{m^2}{2\rho}\right). \tag{3.4}$$

Note that in general the system (3.1) cannot be reduced to a conservation form,

and is in a quasi-conservation form. When $\alpha = 1$ it reverts back to a pure conservation form.

3.b *The Physical Problem*

The physical problem that we shall examine and solve numerically is that considered by Payne [4]. A cylindrical diaphragm of radius r_0 separates the internal fluid from the external one; both are at rest. The conditions in the two regions are homogeneous and the outer pressure and density are higher than the inner ones. The ratio between the initial outer and inner pressure is $p^* > 1$. Similarly $\rho^* > 1$.

At $t = 0$ the diaphragm is removed and a flow begins inward, creating a shock wave. The motion of this collapsing cylindrical shock is not uniform and the axis is a singular point of the solution. We shall be particularly interested in the collapse and rebound motion of the shock.

Note that given p^* and ρ^* we can determine the temperatures. If we take $p^* = \rho^*$ then the two initial regions have equal temperatures. Of course in time the temperature field will also become nonuniform.

3c. *The Dimensionless Equations*

We wish to transform the system (3.1) into a dimensionless form. In order to do this we define the following dimensionless (primed) quantities:

$$r' = r/r_0\,, \qquad \rho' = \rho/\rho_0\,, \qquad p' = p/p_0\,, \qquad u' = u/u_0\,, \qquad t' = t/t_0\,, \tag{3.5}$$

where r_0 is the diaphragm radius; ρ_0 and p_0 are, respectively, the initial density and pressure in the inner region; $u_0 = \sqrt{p_0/\rho_0} = c_0\sqrt{\gamma}$ where c_0 is the initial speed of sound in the inner region; and $t_0 = r_0/u_0$.

Note that unlike Payne we did not take u_0 to be c_0. Had we taken $u_0 = c_0$ the resulting equations would have been similar but not identical to (3.2). As a result the Jacobian $A' = \partial F'/\partial W'$ would have differed from A so that the stability criteria for the primed and unprimed systems would have differed. We elected to take $u_0 = c_0/\sqrt{\gamma}$ thereby causing the new primed system to be identical to (3.2), preserving thusly the matrix A, its eigenvalues and hence the stability condition.

To summarize, we shall use a dimensionless sytem which, after dropping the primes for convenience' sake, is identical to (3.1) and (3.2).

For the various stability criteria that are developed we need the spectral radius of A, i.e., we need to know the eigenvalues. It can be shown that the eigenvalues of A are u, $u \pm c$ where $c = \sqrt{\gamma p/\rho}$ is the speed of sound. Thus $\rho(A) = |u| + c$. In practice therefore we took $\Delta t_n = (\Delta x)\{z(\theta, l)/[\max_j (|u_j^n| + c_j^n)]\}$.

3d. *Initial Conditions*

The initial conditions refer to the dimensionless scheme in which the diaphragm radius is 1. The internal initial pressure and density are also 1, i.e., $\rho_0 = p_0 = 1$.

If we designate the radius by $1 = K\Delta x$, where Δx is the spatial mesh size, we put

$$\begin{aligned} &u_j^0 = 0, \qquad \forall_j\ ; \\ &\rho_j^0 = p_j^0 = 1 \qquad j < K; \qquad \rho_j^0 = \rho^* \qquad \text{and} \qquad p_j^0 = p^*, \qquad j > K. \end{aligned} \tag{3.6}$$

Even though we have not yet defined ρ_K^0, p_K^0 we can still, from (3.3) and the equation of state, write down

$$R_j^0 = r_j\rho_j^0; \qquad M_j^0 = 0; \qquad E_j^0 = \frac{r_j p_j^0}{\gamma - 1}\ ; \qquad \forall_j\ . \tag{3.7}$$

We can thus evaluate R_j^0, M_j^0 and E_j^0 explicitly for all j except for $j = K$. At $j = K$ we shall define ρ_K^0 and p_K^0 in such a way that the resulting E_K^0 and R_K^0 are the arithmetic mean of E_j^0 and R_j^0 for $j = K \pm 1$, thus we find

$$\rho_K^0 = \frac{1}{2}(\rho^* + 1) + \frac{\Delta x}{2}(\rho^* - 1), \tag{3.8}$$

$$p_K^0 = \frac{1}{2}(p^* + 1) + \frac{\Delta x}{2}(p^* - 1). \tag{3.9}$$

3e. *Domain of Solution and Boundary Conditions on the Outside*

The problem as defined above is actually in the semiinfinite domain $0 \leqslant r < \infty$. In practice, however, one must specify a finite domain. It turns out that if the outer boundary is taken at twice the diaphragm radius (i.e., $0 \leqslant r \leqslant 2$) then at $r = 2$ there is very small effect due to the shock collapsing and rebounding from the axis up to the time the rebounding shock returns to the diaphragm location.

Having defined the domain of calculation we have to specify the conditions on $r = 2$ for u, ρ, p, R, M, E. Thus, going from the n-th to the $(n + 1)$-st time step we must specify, for example, $E_{j=2K}^{n+1}$. However E_{2K}^{n+1} must be computed using E_{2K}^n and $E_{2K\pm1}^n$. Thus, in the case of the explicit scheme, if we have l iterations we must use E_{2K}^n, $E_{2K\pm1}^n$, $E_{2K\pm2}^n$,..., $E_{2K\pm l}^n$. The values for $j > 2K$ must be obtained by extrapolation. Using Lagrange interpolation of second order the value of a variable ζ at $(2K + 1, n)$ is given by

$$\zeta_{2K+1}^n = \zeta_{2K-2}^n - 3\zeta_{2K-1}^n + 3\zeta_{2K}^n\,, \tag{3.10}$$

where ζ can be either u, p or ρ. Using previous definitions and the equation of state we also find

$$\begin{aligned} R_{2K+1}^n &= r_{2K+1}\rho_{2K+1}^n = (2 + \Delta x)\,\rho_{2K+1}^n\,, \\ M_{2K+1}^n &= R_{2K+1}^n u_{2K+1}^n\,, \\ E_{2K+1}^n &= \frac{2 + \Delta x}{\gamma - 1} p_{2K+1}^n + \frac{1}{2} M_{2K+1}^n u_{2K+1}^n\,. \end{aligned} \tag{3.11}$$

Note that at $t = 0$ ($n = 0$) the L.H.S. of (3.10) and (3.11) take the proper values given by (3.6) and (3.7).

3f. *Boundary Conditions on the Axis*

While for the outer boundary ($r = 2$) the parabolic extrapolition sufficed, the situation at the axis is more complicated. First it is clear that the following is true at $r = 0$:

$$\begin{aligned} u_0^n &= 0, \\ R_0^n &= [r\rho_0^n]_{r=0} = 0, \\ M_0^n &= R_0^n u_0^n = 0, \\ E_0^n &= \left[r \frac{p_0^n}{\gamma - 1}\right]_{r=0} + \frac{1}{2} M_0^n u_0^n = 0. \end{aligned} \tag{3.12}$$

In addition, we'll need the quantities p, ρ and E/R at the axis. All these three quantities formally are of the form % at the axis. In order to compute them we first thought of a simple extrapolation from $r = \Delta x, 2\Delta x, 3\Delta x$ to $r = 0$. This method failed; this is so because as the shock nears the axis we get very high gradients at that region and the smoothness required for a valid extrapolation is not available. We tried another method which was successful. We present it herein[2]:

Consider the hydrodynamic equation of continuity in its integral form

$$\frac{\partial}{\partial t} \int_{V(t)} \rho \, dV + \oint_{S(t)} \rho \cdot (\mathbf{u} \cdot d\mathbf{S}) = 0, \tag{3.13}$$

where $S(t)$ is a surface which at time t encloses a volume $V(t)$. If $S(t)$ describes a right cylinder of radius $r_i = i\Delta x$ and height h, and if the flow has cylindrical symmetry, i.e., $\mathbf{u} = \hat{r}u$ where $\hat{r}$ is the radial unit vector then we can rewrite (3.13) as

$$\frac{\partial}{\partial t} \int_0^{r_i^2} \rho(\sqrt{\xi}, t) \, d\xi + 2r_i \rho(r_i, t) \, u(r_i, t) = 0, \tag{3.14}$$

where $\xi = r^2$. We shall evaluate the integral in such a way that $\rho(0, t)$ will appear explicitly. Evaluating the integral in (3.14) with the trapezoidal method, we have

$$\int_0^{r_i^2} \rho(\sqrt{\xi}, t) \, d\xi \approx \tfrac{1}{2}[\rho(0, t) + \rho(r_i, t)](r_i^2 - 0) = \tfrac{1}{2}[\rho(0, t) + \rho(r_i, t)] \, r_i^2$$

and the error, assuming the integrand to be $C^2[0, r_i]$, is $O[(r_i^2)^3]$, i.e., $O(r_i^6)$ which

[2] Payne [4] had the same starting point. We were unable, however, to reproduce his formulation.

is more than sufficient for our purposes if $r_i = O(\Delta x)$. Indeed, taking $r_i = \Delta x$ Eq. (3.14) becomes

$$\frac{\partial}{\partial t}\left\{\frac{1}{2}\left[\rho(0, t) + \rho(\Delta x, t)\right](\Delta x)^2\right\} + 2\Delta x\, \rho(\Delta x, t)\, u(\Delta x, t) = 0. \tag{3.15}$$

The numerical estimate of $\partial/\partial t\,[\rho(0, t)]$ and $\partial/\partial t[\rho(\Delta x, t)]$ can be centered either around $n\Delta t$ or $(n + \frac{1}{2})\,\Delta t$. In both cases the error is of $O(\Delta t^2)$. However, in the first case we will have ρ_0^{n+1} depending on ρ_0^{n-1} while in the second case ρ_0^{n+1} will depend on $\rho_0{}^n$. Since we may expect at the time of the shock coalescence strong timewise gradients it is preferable to rely on information which is as "late" as possible. We thus get, centering all of (3.15) around $(n + \frac{1}{2})\,\Delta t$,

$$\frac{1}{2}\left[(\rho_0^{n+1} - \rho_0{}^n) + (\rho_1^{n+1} - \rho_1{}^n)\right]\frac{(\Delta x)^2}{\Delta t} + \frac{2(\Delta x)}{4}(\rho_1{}^n + \rho_1^{n+1})(u_1{}^n + u_1^{n+1}) = 0$$

or

$$\rho_0^{n+1} = \rho_0{}^n + \rho_1{}^n - \rho_1^{n+1} - \lambda(\rho_1{}^n + \rho_1^{n+1})(u_1{}^n + u_1^{n+1}). \tag{3.16}$$

In order to evaluate the energy on the axis consider the integral form of the energy equation

$$\frac{\partial}{\partial t}\int_{V(t)} e\, dV + \oint_{S(t)} (e + p)(\mathbf{u} \cdot d\mathbf{S}) = 0. \tag{3.17}$$

Using the same development as the one that follows (3.13) we finally obtain

$$e_0^{n+1} = e_0{}^n + e_1{}^n - e_1^{n+1} - \lambda(e_1{}^n + e_1^{n+1} + p_1{}^n + p_1^{n+1})(u_1{}^n + u_1^{n+1}). \tag{3.18}$$

From (3.16) and (3.18) we can find $(E/R)_0^{n+1} = (e/\rho)_0^{n+1}$ and $p_0^{n+1} = (\gamma - 1)\, e_0^{n+1}$.

It should be remarked that we also tried integration formulas more elaborate than the trapezoidal method. No significant improvement in the actual numerical results was found.

Until the shock converges upon the axis $u(\Delta x, t) \leqslant 0$. Since $u_0{}^n = 0$ for all n we shall say that the shock reached $r = 0$ at $t_c = \sum_{m=1}^{n+1} \Delta t_m$, where $(n + 1)$ is the first natural number for which $u_1^{n+1} > 0$.

3g. *Numerical Results*

3g. 1 *General Remarks*

The numerical results are presented graphically in Figs. 1–9. Figure 1 is the pressure distribution at various times as predicted by the explicit Lax–Wendroff scheme. Figure 2 shows the results of using the internal iterative scheme. The rest

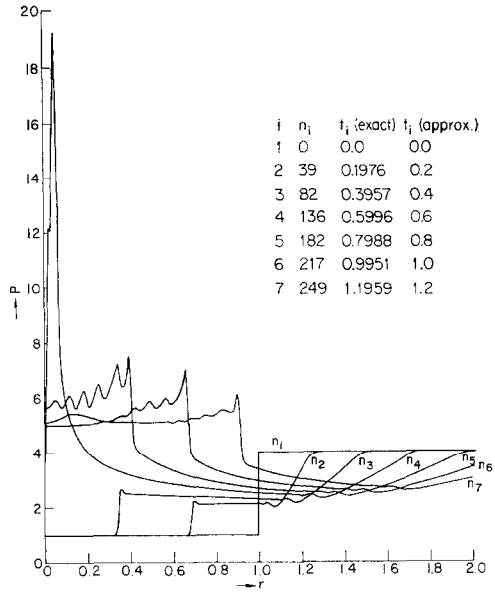

FIG. 1. Pressure vs radius (Explicit Scheme), given for approximately every 0.2 time units; $\gamma = 1.4, p^* = \rho^* = 4, K = 100$ ($\Delta x = 1/K = 10^{-2}$).

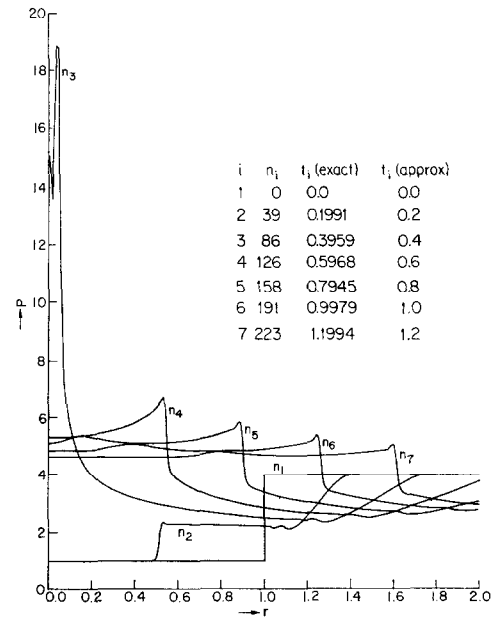

FIG. 2. Pressure vs radius (Internal Iterative Scheme), given for approximately every 0.2 time units; $\gamma = 1.4, p^* = \rho^* = 4, K = 100, \theta = 0.5, l = 2$ (1 iteration).

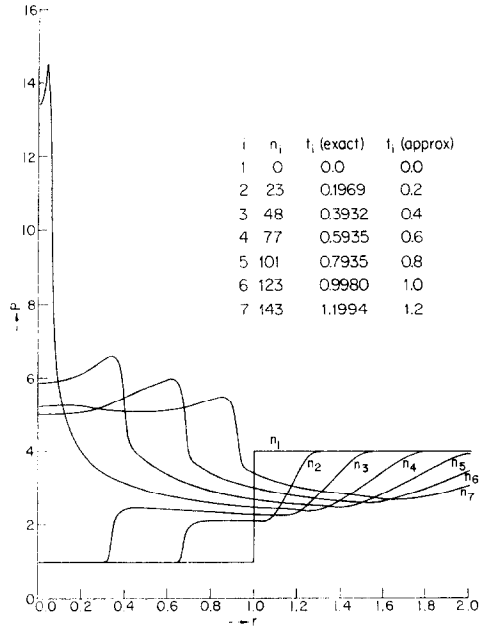

FIG. 3. Pressure vs radius (External Iterative Scheme), given for approximately every 0.2 time units; $\gamma = 1.4, p^* = \rho^* = 4, K = 100, \theta = 0.2, l = 2$.

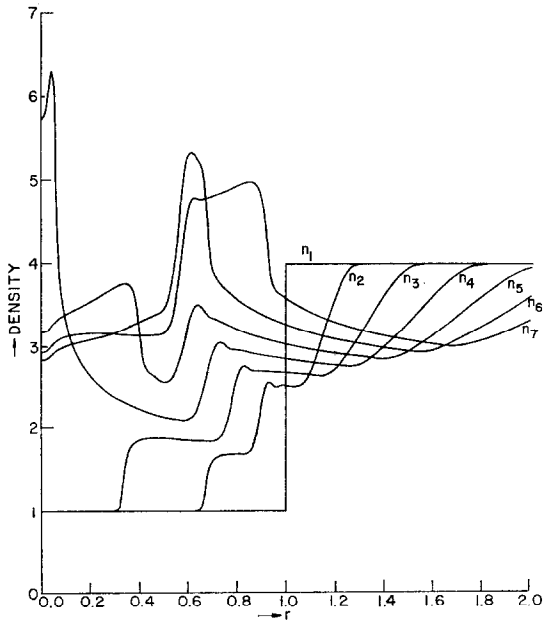

FIG. 4. Density vs radius (External Iterative Scheme), given for approximately every 0.2 time units; all parameters and exact times are the same as in Fig. 3.

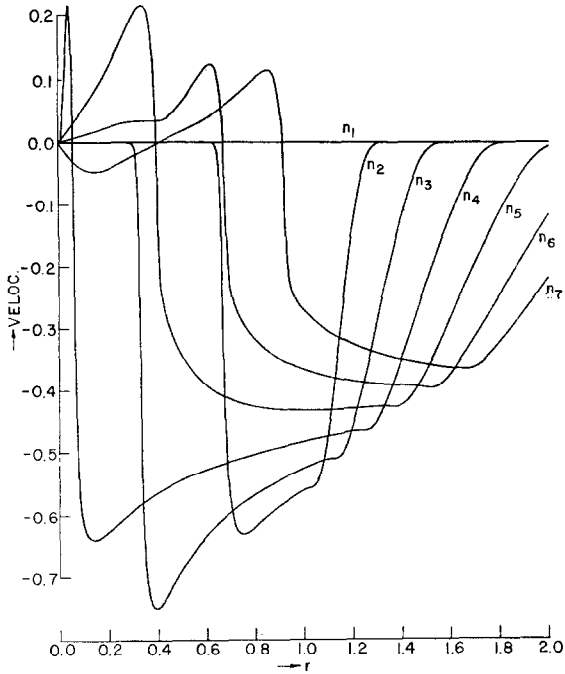

FIG. 5. Velocity vs radius (External Iterative Scheme), given for approximately every 0.2 time units; all parameters and exact times are the same as in Fig. 3.

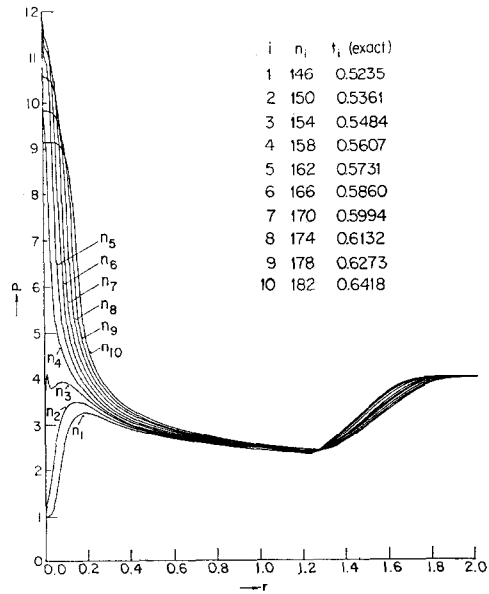

FIG. 6. Pressure vs radius for times near shock convergence into axis (External Iterative Scheme); $\gamma = 1.4, p^* = \rho^* = 4, K = 100, l = 2, \theta = 1.0$.

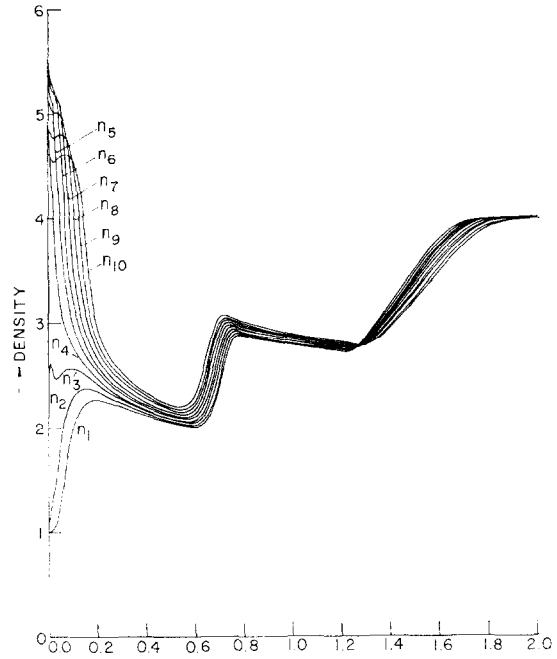

FIG. 7. Density vs radius for time near shock convergence unto axis (External Iterative Scheme); all parameters and exact times are the same as in Figure 6.

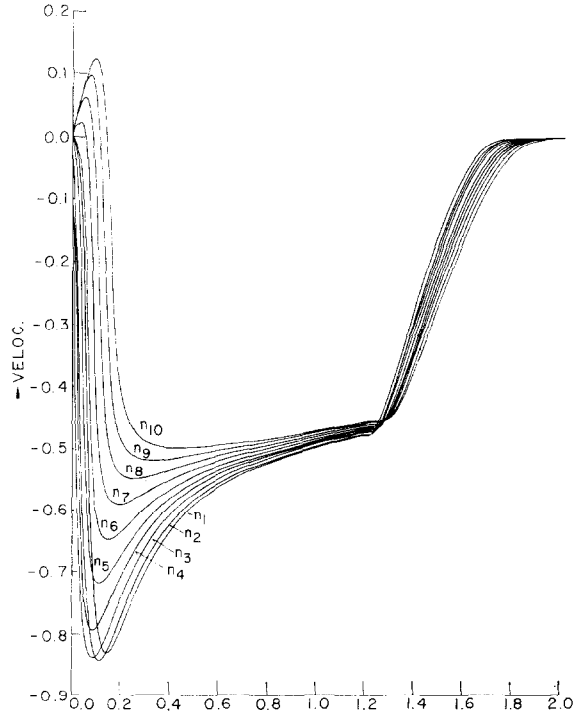

FIG. 8. Velocity vs radius for time near shock convergence unto axis (External Iterative Scheme); all parameters and exact times are the same as in Figure 6.

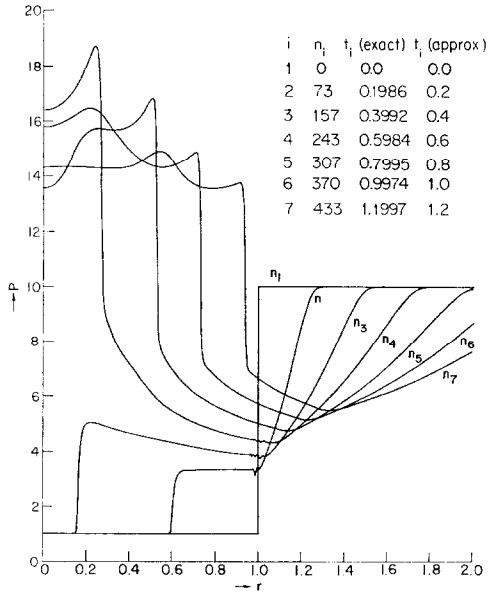

FIG. 9. Velocity vs radius (External Iterative Scheme); given for approximately every 0.2 time units; $\gamma = 1.4$, $p^* = \rho^* = 10$, $K = 200$; $\theta = 0.3$; $l = 2$.

are for the external iterative schemes for various values of θ, $K = 1/\Delta x$, p^* and ρ^*; in all of them $\gamma = 1.4$ and $l = 2$.

It was found that in general the overall trend of the results agrees with those given by Payne [4]. There are, however, some major differences, such as for example, the time for the shock to reach the axis. A more detailed comparison will be given later.

3g. 2 *Dependence of the Numerical Results on the Various Schemes and Parameters*

In addition to the physical character and significance of the results (which Payne [4] discusses at length) it is desirable to consider several points which bear upon the sensitivity of the results to, and their dependence on, the various methods of calculation, the magnitude of the controlling parameters, etc. These points are worthwhile considering because they are of importance not only for the specific physical physical problem solved here but also for other problems which may be attacked using similar methods.

(*i*) *The difference schemes.* In Section 2 we talked about three difference schemes given by Eqs. (2.4), (2.15) and (2.17). The explicit Lax–Wendroff-like scheme, (2.4), is found to contain many numerical oscillations which are much more detrimental

than in the slab symmetry case, especially as the shock converges towards the center; see Fig. 1. We abandoned the use of this explicit scheme.

It remains to compare the two iterative schemes—the external and internal ones, Eqs. (2.15) and (2.17), respectively. When $\theta = 1$, the two schemes are identical. When $\theta < 1$ the external scheme yielded much smoother results. This is particularly so when $\theta < 1/2$ where the internal scheme gave worse results than the explicit one. We then checked this phenomenon in the slab symmetry case ($\psi = 0$) for $\theta = 0.2$ and $\theta = 0.3$ and found the external scheme to yield good smooth results while the internal scheme led to nonlinear instabilities.

Another major difference between the two iterative schemes is the predicted time for the shock to reach the axis (convergence time $= t_c$). First, the external iterative scheme, for given initial conditions, predicted the same convergence time, to within 2%, for all θ's and all l's (number of iterations). On the other hand, the internal scheme gave widely different t_c's for different θ's, all of them being lower than the ones predicted by the external scheme. Of course, when $\theta = 1$ they both give the same result which also agrees with the convergence time predicted by the explicit Lax–Wendroff scheme. It is well known that while Lax–Wendroff–like schemes produce post-shock oscillations they do predict the correct shock speed. As an illustration of the differences among the methods consider the case of $p^* = \rho^* = 4$, $\gamma = 1.4$, $K = 100$: the time to reach the axis as given by the explicit scheme or the external iterative one, for all θ, is $t_c = 0.57$; on the other hand, the internal iterative scheme predicts $t_c = 0.38$ for $\theta = 0.5$ and $t_c = 0.46$ for $\theta = 0.2$.

In view of all that is said above we decided to concentrate on utilizing the external scheme [Eq. (2.15)].

(ii) *Stability condition.* The actual stability criteria turned out in practice to be the theoretical ones given in Section 2 with the equality sign taken rather than the inequality. If the time steps exceed the maximum allowed by the linear theory then strong linear instabilities appear. Reducing the time step does not serve any purpose; on the contrary, if Δt is too small, weak (nonlinear) instabilities occur, confirming the same phenomenon as observed by Richmyer and Morton in the slab-symmetry case [8].

(iii) *Efficacy of the external scheme vis-a-vis different initial conditions and the parameters l, γ, K and θ.* The numerical results covered the following ranges of initial conditions: weak shock ($\rho^* = p^* = 1.5$); intermediate-strength shock ($\rho^* = p^* = 4$); and strong shock ($p^* = \rho^* = 10$). In all cases we used both $\gamma = 1.4$ and $\gamma = 3$. The values of θ tested were 0.2, 0.3, 0.5, 0.75, 1.0 and 1.5. The mesh size was taken to be: $K = 50$, 100, 200 and 400. Various numbers of iteration l were tried.

As expected the post-shock oscillations were more problematical the stronger the shock.

A general observation of importance is that one iteration ($l = 2$) suffices to smooth out the numerical noise. As a matter of fact increasing l causes in the very beginning, worsening of the phenomenon which, however, is damped out very rapidly with time. As a result the numerical solution for $l > 2$ looks the same as for $l = 2$. Thus it is possible to save computer time by using $l = 2$.

Another interesting phenomenon is the fact that as θ increases toward 1,[3] the numerical system becomes more dissipative in the following sense: The shock waves are spread over a larger number of cells and the local extrema of the pressure, velocity and density profiles become less pronounced. When the shock is away from the axis these differences are very small; as the shock converges to $r = 0$ the resulting differences are significant. For an illustrative example, see Table I in which we list the maximum values of pressure and density for the case $\rho^* = p^* = 4$, $\gamma = 1.4$, $K = 100$ at two times: $t = t_c \sim 0.57$ (time when shock converges upon the axis) and $t \sim 1$, at which time the rebounding shock has diverged from the axis and is a considerable distance out (in all cases $l = 2$; i.e., one iteration):

TABLE I

Maximum Values of Pressure and Density[a]

$r_s = 0$ $t \sim 0.57$			$r_s \sim 0.62$ $t \sim 1.0$			$p^* = \rho^* = 4$			
$\theta = 1.0$	$\theta = 0.5$	$\theta = 0.2$	$\theta = 1.0$	$\theta = 0.5$	$\theta = 0.2$	$K = 100$	$\gamma = 1.4$	$l = 2$	
11.9258	16.5811	27.6607	5.8405	5.9271	5.9872		$p_{\max}$		
5.6085	7.0540	9.7167	5.1376	5.2745	5.3622		$\rho_{\max}$		

[a] Conditions: $\rho^* = p^* = 4$, $\gamma = 1.4$, $K = 100$ at $t = t_c \sim 0.57$; $t \sim 1$.

As we remarked, as θ increases the results are more dissipative in the above sense. Since increasing θ means giving more weight to the iterative member of the scheme (2.15), we deduce that it is indeed the iterations that cause the dissipation. At the same time it must be emphasized that this kind of dissipation does not imply a smoother profile near the shock. On the contrary, smaller θ's yield results with less numerical noise. A plausible explanation for this seeming "paradox" is the following: The iterative and noniterative terms of the finite difference scheme have, respectively, the weights of θ and $1 - \theta$. The numerical domain of dependence of the iterative term, for $l = 2$, is $4\Delta x$ while for the noniterative terms it is $2\Delta x$.

[3] When $\theta > 1$, say $\theta = 1.5$, we encountered very strong oscillations in the regions of large gradients.

Thus the "weighted-average" of the two is

$$\theta(4\Delta x) + (1 - \theta)(2\Delta x) = (1 + \theta)\, 2\Delta x. \tag{3.19}$$

Let us recall now that the stability criterion for $l = 2$ and $0.17 = \theta_0(2) < \theta < \frac{1}{2}$ is $\Delta t \leqslant \Delta x/[\rho(A)\sqrt{2\theta}]$ from which we deduce that the numerical domain of dependence necessary for stability is $2(\Delta x/\sqrt{2\theta})$.[4] Now if the "weighted-average" domain [Eq. (3.19)] indeed represents the "actual" domain of dependence then we must require it, for reasons of stability, to be smaller than $2(\Delta x/\sqrt{2\theta})$. Hence we have the inequality

$$2(1 + \theta)\, \Delta x \leqslant 2\Delta x/\sqrt{2\theta}. \tag{3.20}$$

On the other hand, we would like to maximize the time step (for the reasons mentioned in Section 3g.2 (ii)). This implies that in (3.20) we must choose the equality sign and we get

$$\sqrt{2\theta}\,(1 + \theta) = 1. \tag{3.21}$$

The solution of (3.21) is $\theta = 0.299 \approx 0.3$ and indeed $\theta = 0.3$ gives the smoothest results, particularly in the cases of strong shocks ($p^* = \rho^* = 10$).

The last point to be checked is that concerning the effect of mesh size. As K increases ($K = 1/\Delta x$), the post-shock oscillations become smaller. Since the shock is spread on the same number of cells the shock profile in the physical coordinates is much steeper for larger K. Values at the axis at the time of shock convergence increase with K—this is to be expected because the hydrodynamic variables behave as $1/\Delta x$ near $r = 0$. However, qualitatively the results near the axis are the same for all $K \geqslant 50$ while away from $r = 0$ the results are almost independent of K (within the limits of accuracy desired).

(iv) *Comparison with previous results.* As indicated in Section 3g.1 the general trend of the results agrees with those given by Payne [4], but we mentioned the different arrival time of the shock at the axis. Thus while we predict, based on both the Lax–Wendroff and the iterative scheme, $t_c \approx 0.57$ for $p^* = \rho^* = 4$ and $\gamma = 1.4$, Fig. 1 in Ref. [4] indicates a convergence time of 0.66. There are other differences which might be summarized as follows: the shock locations at various times and the extremum hydrodynamic values associated with them, are self-consistent when predicted by our external iterative scheme for all values of θ, K (mesh size) and l (number of iterations). They do, however, differ markedly from the results given in Ref. [4].

[4] The slope of the one sided domain of dependence is indeed $1/\rho(A) = 1/|u| + c = \Delta t/(\Delta x/\sqrt{2\theta})$. However, the numerical domain of dependence is symmetric and is twice $(\Delta x/\sqrt{2\theta})$.

REFERENCES

1. P. LAX AND B. WENDROFF, *Commun. Pure Appl. Math.* **13** (1960), 217–237.
2. J. L. ANDERSON, S. PREISER, AND E. L. RUBIN, *J. Comput. Phys.* **2** (1968), 279–287.
3. D. D. HOUGHTON AND A. KASAHARA, *Commun. Pure Appl. Math.* **21** (1968), 1–23.
4. R. B. PAYNE, *J. Fluid Mech.* **2** (1957), 185.
5. S. ABARBANEL AND G. ZWAS, *Math. Comp.* **23** (107) (1969), 549.
6. H. O. KREISS, *Nordisk Tidskr. Information-Behandling* **2** (1962), 153.
7. G. STRANG, *Num. Math.* **6** (1964), 37–46.
8. R. D. RICHTMYER AND K. W. MORTON, "Difference Methods for Initial-Value Problems," 2nd ed., Chap. 12. Interscience, New York, 1967.